URSI GASS 2020, Rome, Italy, 29 August - 5 September 2020

Experimental Validation of a 3D Microwave Imaging Device for Brain Stroke Monitoring.

Jorge A. Tobon V.*(1), Lorenzo Crocco(2), and Francesca Vipiana(1)
(1) Department of Electronics and Telecommunications, Politecnico di Torino, 10129 Turin, Italy, e-mails: jorge.tobon@polito.it, francesca.vipiana@polito.it
(2) Institute for the Electromagnetic Sensing of the Environment, National Research Council of Italy, 80124 Naples, Italy, e-mail: crocco.l@irea.cnr.it

Abstract

In this work we present the experimental validation of a 3D microwave imaging device to brain observation. The device is conceived as a way to monitor stroke development, supporting physicians in the follow-up of patients in the aftermath of cerebrovascular accidents, and giving to them extra information for decision-making and application of therapies. The device acquires data through antennas placed around the patient head, in a low-complexity system that guarantees that available information is enough for reliable outcome. Experimental testing is performed on a 3-D human-like head phantom with promising results.

1 Introduction

Brain stroke, with over 5 million deaths each year [1] and several permanent injures as consequences for the surviving patients, is an issue of crucial importance nowadays. A rapid diagnosis and a continuous monitoring of the disease leads to a fast and proper reaction of the physicians, with an improvement of the patient conditions and better prognosis.

Already assessed technologies (Magnetic Resonance Imaging (MRI) or X-ray based Computerized Tomography (CT)) are used to obtain diagnostics based on images, but with some drawbacks relative to cost and availability in emergency situations (MRI), ionizing radiation that difficults the repetition (CT), and bulky equipment (both) that make them not suitable for a continuous monitoring in ambulance or as bedside devices.

In this scenario microwave imaging (MWI) techniques appear as a complementary tool to the already adopted technologies, covering areas as pre-hospital check, discrimination of type of stroke (ischemia or hemorrhage), continuous monitoring and bedside imaging. MWI avoids the ionizing radiations of X-rays, permitting a continuous and repeated application of low-power useful signals. Broad availability of microwave off-the-shelf sensors and devices facilitates building and miniaturization of the final devices [2], and low-cost acceleration is also feasible [3].

In the last few years some devices for MWI in this particular application has been presented [4, 5, 6]. Two of the most prominent of these devices have two different approaches: to classify between ischemic and hemorrhagic stroke comparing acquired data to a data base of already examined patients [4], with no images as outcome and to make the quantitative image of the brain characteristics [5] with increases in complexity, size of the device and computation time. Recently, a more compact and low-complexity system was presented in [6], its objective is to generate an image of the brain disease, but still following a 2-D approach.

In this work we present the experimental validation of a low-complexity, fast and 3D system that creates an image of the stroke affected region. We focus in a continuous monitoring device that create an image of a "small" variation taking place in a localized point, without the goal of reconstructing the complete brain structure. This choice permits us to keep the low complexity, and to achieve real-time image generation, as Born approximation for scattering is applied. We adopt a differential imaging approach where data at two different times are used together with fast algorithms for imaging based on distorted Born approximation [7, 8]. Differential data reflects only the variation due to the development of the stroke in time.

In the following we briefly summarize the system structure and its validation through a 3d experimental tests.

2 System Description

The proposed system is composed by three main hardware sub-systems: the helmet with the sensors, the switching matrix, and the signal acquisition device. Figure 1 depicts the complete hardware system. A rigorous procedure was adopted to design the device and to guarantee a quantity of information able to reconstruct a 3D image of the region of interest [8].

The signal acquisition is performed by a standard Vector Network Analyzer (VNA) (Keysight N5227A, 10 MHz-67 GHz, input power is set to 0 dBm and IF filter to 10 Hz) working a signal generator and receiver.

The switching matrix is the interface between the antennas on the head and the VNA. As described in [9], it has been

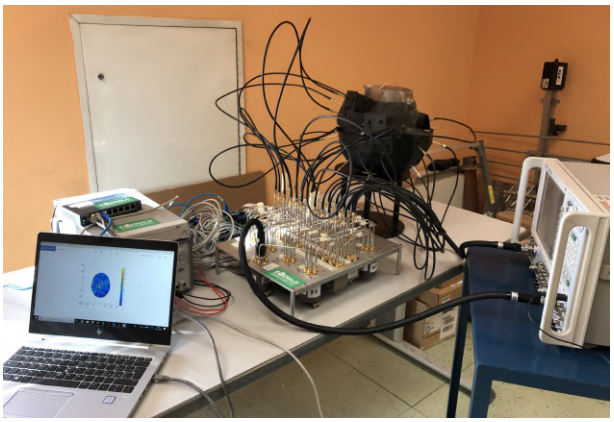

Figure 1. Complete system with antennas' helmet, switching matrix, VNA, and control/imaging computer

designed to have 24 paths from each antenna to both of the VNA ports, permitting each antenna to work as transmitter and as receiver. Electrical length of all the paths is the same, avoiding different phase shifting in each channel.

The antennas helmet is an array of 24 printed monopole antennas disposed conformly to the head surface, and kept in position by a 3D-printed wearable helmet. The quantity and position of antennas are determined by rigorous procedure proposed in [8]. A box of graphite-silicon material is used around each antenna to both mechanical support and signal matching, making a modular array where antennas can be changed and removed easily. The use of a flexible and solid material is an advantage respect to matching liquids in terms of handling, portability, system operation, repeatibility and patient comfort.

The software side of the system relies mainly in the linearized reconstruction of the target. The localized and small dimension of the object permits to apply the Born approximation, that leads to a linear relationship:

$$\Delta S(r_p, r_q) = \mathscr{S}(\Delta\chi) \tag{1}$$

between ΔS (differential of measured scattering matrices) and $\Delta\chi$ (contrast due to the target presence). The linear compact integral operator $\mathscr{S}$ yields in the kernel $-j\omega\varepsilon_b/4\,E_\mathrm{b}(r_m, r_p)\cdot E_\mathrm{b}(r_m, r_q)$, with r_m the points in the imaging domain D, r_p and r_q the positions of the transmitting and receiving antennas. $\omega = 2\pi f$ is the angular frequency, and j the imaginary unit. E_b is the field radiated on the domain D with no presence of any target or disturbance. These E_b fields are obtained through a in-house developed 3D Finite Element Method (FEM), considering the complete and realistic geometry of the system.

A strong and recognized method to do the inversion of equation 1 is the truncated singular value decomposition (TSVD) scheme [10], which obtains the unknown differential contrast through the inversion:

$$\Delta\chi = \sum_{n=1}^{L_t} \frac{1}{\sigma_n} \langle \Delta S, [u_n] \rangle [v_n], \tag{2}$$

applying a Singular Value Decomposition on the discretized operator $\mathscr{S}$ (with $\langle [u], [\sigma], [v] \rangle$ being the resultant decomposition). A proper trade-off between accuracy and stability is achieved through the selection of the index L_t, which acts as a regularization parameter.

3 Experimental Validation

The deviced is tested on a human-like phantom of the head, as seen inside the helmet in Fig. 1. The phantom is realized by additive manufacturing from a stereo-lithography (STL) file derived from MRI scans, and is filled with a liquid mixture (made by Triton x-100, water, common salt) that mimics characteristics of average value of different brain tissues [11].

As target to be detected we use a 1.25-cm-radius plastic immersed in the brain-mimicking liquid. This test intends to validate the capacities of the prototype device, identifying the 3-D shape and position of the inserted sphere. It is important to notice that plastic sphere, used by simplicity, is not mimicking a hemorrhage or cloth, but simulates a dielectric contrast comparable to the case of interest.

The differential approach discussed before leads to perform 2 measurement sets at different times. The first set is in the absence of the target, while in the second one the sphere is inserted inside the phantom. In each case a 24×24 scattering matrix is obtained, and their difference is used as input to the linearized algorithm (TSVD). Results shown in the following are relative to one of the tests performed in validation phase. The differential scattering matrix is depicted in Fig. 3(a), self elements are not depicted because not used in currently in our reconstruction scheme. The absence of the self elements permits us to see the range variation in the measured transmission coefficients. Measured signals are above -100 dB, that means that useful data is above noise floor for the VNA in the experiment conditions (-110 dBm at 1GHz, IF filter equal to 10 Hz with 0 dBm of transmitted signal). The symmetry of the matrix was expected and confirms the reciprocity of the system. Figure 3 (b,c) shows 2 cuts obtained from the 3D resulting image from TSVD processing. Both cuts are centered at the detected sphere, and expected position and dimension are showed as a red circle. A good correspondence between expected and detected size and position is demonstrated in these images. Figure 3 (d) reproduce a rendering of the localized target, keeping data above -3 dB in the normalized differential contrast, and confirming that shape and dimension of the obtained reconstruction match the expected object.

A total scan to acquire the measurement data requires less than 4 minutes with the current prototype. The TSVD algorithm takes less than 1 second to generate an image, the computational cost is negligible with respect to measurement time. These times are compatible with the continuous monitoring application.

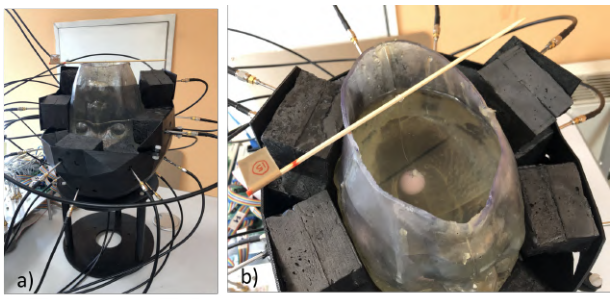

Figure 2. (a)Detail of the helmet-phantom subsystem; (b): Experimental set-up

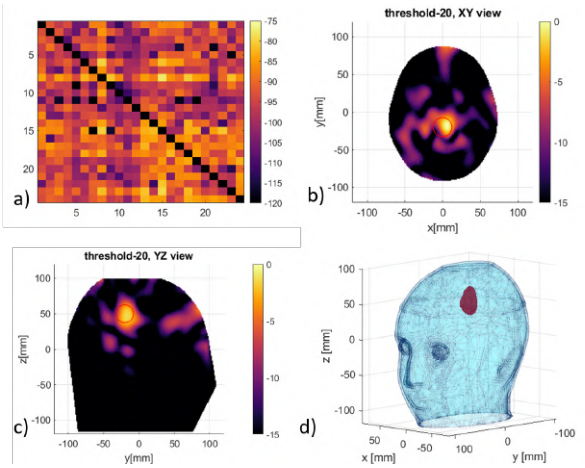

Figure 3. Differential scattering matrix in dB (a) given as input to TSVD generates 3D reconstructions, from which (b)-(c) are 2 cross-sections at sphere center; and (d) show the 3-D rendering of the imaged stroke.

4 Conclusions and Perspectives

A 3D microwave imaging device for monitoring of brain stroke is presented and described in this work. The design of the device followed a rigorous method to assure that system would reconstruct an unknown target through scattering matrix measurements, as demonstrated later with the here presented experimental validation.

Next activities relative to this research will test the implemented device in a more realistic situation, adding the other brain tissues to the human-like phantom.

5 Acknowledgements

This work was supported by the Italian Ministry of University and Research under the PRIN project "MiBraScan - Microwave Brain Scanner for Cerebrovascular Diseases Monitoring."

References

[1] E. J. Benjamin, P. Muntner, and M. S. Bittencourt, "Heart disease and stroke statistics-2019 update: a report from the american heart association," *Circulation*, vol. 139, no. 10, pp. e56–e528, 2019.

[2] M. R. Casu, M. Vacca, J. A. Tobon Vasquez, A. Pulimeno, I. Sarwar, R. Solimene, and F. Vipiana, "A cots-based microwave imaging system for breast-cancer detection"," *IEEE Trans. Biomed. Circuits Syst.*, vol. 11, no. 4, pp. 804–814, Aug. 2017.

[3] I. Sarwar, G. Turvani, M. R. Casu, J. A. Tobon Vasquez, F. Vipiana, R. Scapaticci, and L. Crocco, "Low-cost low-power acceleration of a microwave imaging algorithm for brain stroke monitoring," *J. Low Power Electron.s Appl.*, vol. 8, no. 4, 2018. [Online]. Available: http://www.mdpi.com/2079-9268/8/4/43

[4] A. Fhager, S. Candefjord, M. Elam, and M. Persson, "Microwave diagnostics ahead: Saving time and the lives of trauma and stroke patients," *IEEE Microwave Mag.*, vol. 19, no. 3, pp. 78–90, May 2018.

[5] M. Hopfer, R. Planas, A. Hamidipour, T. Henriksson, and S. Semenov, "Electromagnetic tomography for detection, differentiation, and monitoring of brain stroke: A virtual data and human head phantom study." *IEEE Antennas Propag. Mag.*, vol. 59, no. 5, pp. 86–97, Oct. 2017.

[6] A. S. M. Alqadami, K. S. Bialkowski, A. T. Mobashsher, and A. M. Abbosh, "Wearable electromagnetic head imaging system using flexible wideband antenna array based on polymer technology for brain stroke diagnosis," *IEEE Trans. Biomed. Circuits Syst.*, vol. 13, no. 1, pp. 124–134, Feb. 2019.

[7] R. Scapaticci, O. Bucci, I. Catapano, and L. Crocco, "Differential microwave imaging for brain stroke follow up," *Int. J. Antennas Propag.*, vol. 2014, no. Article ID 312528, p. 11 pages, 2014.

[8] R. Scapaticci, J. A. Tobon Vasquez, G. Bellizzi, F. Vipiana, and L. Crocco, "Design and numerical characterization of a low-complexity microwave device for brain stroke monitoring," *IEEE Trans. Antennas Propag.*, vol. 66, pp. 7328–7338, Dec. 2018.

[9] J. A. Tobon Vasquez, R. Scapaticci, G. Turvani, G. Bellizzi, N. Joachimowicz, B. Duchêne, E. Tedeschi, M. R. Casu, L. Crocco, and F. Vipiana, "Design and experimental assessment of a 2D microwave imaging system for brain stroke monitoring," *Int. J. Antennas Propag.*, no. Article ID 8065036, p. 12 pages, 2019.

[10] M. Bertero and P. Boccacci, *Introduction to Inverse Problems in Imaging*. Inst. Phys., Bristol, U.K., 1998.

[11] N. Joachimowicz, B. Duchêne, C. Conessa, and O. Meyer, "Anthropomorphic breast and head phantoms for microwave imaging," *Diagnostics*, vol. 85, no. 8, pp. 1–12, Dec. 2018.